Measurement of Three Dimensional Residual Stresses in Rolled Clad Plates and Welded Joints of a Chemical Tank Structure†

MA Ninshu *, MURAKAWA Hidekazu, LUO Yu*** and DENG Dean****

Abstract

To evaluate the safety of welded joints in a chemical tank before manufacture, the rolling residual stress in steel plates and welding residual stress in welded joints need be measured. In this paper, firstly, the rolling residual stresses in a stainless plate (SUS304) and a clad plate (SUS304/MB410) used in a chemical tank are measured. Then, the welding residual stresses in a simple bead-on-plate weld and a practical filled weld are measured by the inherent strain method. Lastly, the total residual stresses in the welded joints are discussed.

KEY WORDS: (Three Dimensional Residual Stress), (Rolled Clad Plates), (Measurement)

1. Introduction

Clad steel is widely used in pressure vessels and chemical tanks because it has advantages of both the strength and resistance to corrosion. On the other hand, since the base metal and the clad metal have different physical and mechanical properties, residual stresses are often induced by the cladding process and the following welding process. The residual stresses may induce interface peeling at the clad plates, fatigue cracking, stress corrosion cracking during service.

Figure 1 shows a chemical tank in which stainless steel (SUS304), high strength steel (MB410) and thermally rolled clad steel (SUS304/MB410) are used.

Before production, residual stresses in a fillet welded joint, shown in **Fig. 1**, need to be measured. In this paper, firstly, the rolling stresses in both a stainless steel plate (SUS304) and a clad steel plate (SUS304/MB410) are carried out by the layer removal method[1] and conventional stress release method. Then, the residual stresses in a simple bead-on-plate weld and in a practical fillet joint with a clad plate are measured based on the inherent strain method[2-10]. Lastly, the total residual stress states are discussed.

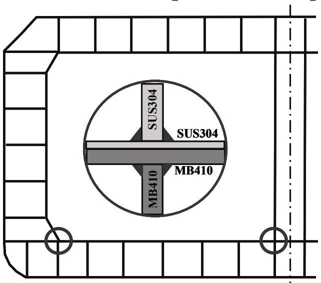

Fig. 1 A chemical tank and welded joints with clad plates

2. Measurement of rolling stress in a stainless plate and a clad plate

2.1 Measurement specimens

Figures 1 and **2** show a stainless plate (SUS304) and a clad plate (SUS304/MB410) made by thermal rolling. The thicknesses of the SUS304 layer and MB410 layer of the clad plate are 3mm and 15mm, respectively. The Young's modulus and Poisson's ratio for SUS304 and MB410 are 198000MPa, 0.28 and 206000MPa, 0.3, respectively.

The rolling stress has two components σ_x and σ_y, which are parallel and perpendicular to the rolling direction, respectively, as shown in **Figs. 2-3**. By cutting off two thin specimen Lx and Ly, two stress components σ_x and σ_y can be separated. The stresses in specimen Lx and in specimen Ly are described by σ_{Lx} and σ_{Ly}. The rolling stresses (σ_x, σ_y) in the original clad plate can be calculated from the stresses (σ_{Lx}, σ_{Ly}) in specimen (Lx, Ly) by **Eq. (1)**,

$$\sigma_x = \frac{\sigma_{Lx} + \upsilon\sigma_{Ly}}{1-\upsilon^2}, \ \sigma_y = \frac{\sigma_{Ly} + \upsilon\sigma_{Lx}}{1-\upsilon^2} \quad (1)$$

where υ is Poisson's ratio.

† Received on December 18, 2009

* Guest Associate Professor
** Professor
*** Professor, Shanghai Jiaotong University
**** Professor, Chongqing University

Transactions of JWRI is published by Joining and Welding Research Institute, Osaka University, Ibaraki, Osaka 567-0047, Japan

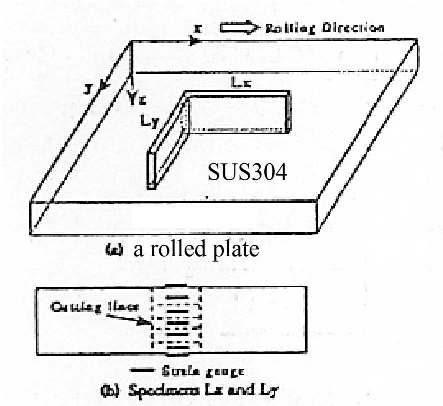

Fig. 2 Specimens of SUS304 plate

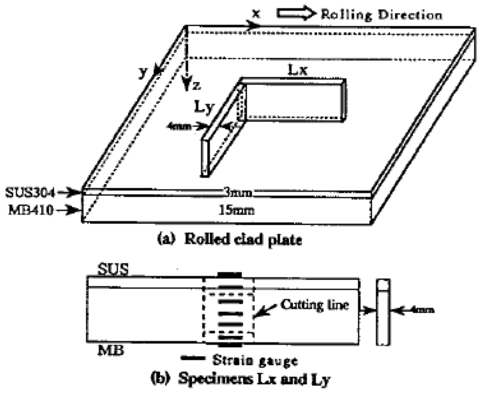

Fig. 3 Specimens of SUS304/MB410 plate

If localized stress distribution at the cladding interface is neglected, the rolling stresses σ_{Lx} and σ_{Ly} can be directly measured using strain gauges attached on specimens Lx and Ly shown in **Fig. 2(b)** and **Fig. 3(b)** by the conventional mechanical stress release method. To measure the local stress and detail distribution through the thickness of the clad plate, a layer removal method is employed for specimens Lx and Ly, which will be described in detail below.

2.1 Rolling residual stresses measurement by layer removal method

(1) Assumption

If it is assumed that the stress in specimen Lx or Ly distributes uniformly in the longitudinal direction and varies only in the thickness direction (z), as shown in **Fig. 4**, the elastic beam theory can be applied to estimate the residual stresses.

(2) Measuring procedure

Step 1: A strain gauge is attached to the specimen Lx and Ly at the position z_m near the lower surface shown in **Fig. 4**.

Step 2: Thin layers with 0.2mm are removed by milling gradually from the SUS304 side. During milling, a cooling oil is used to prevent the temperature rising.

Step 3: After each layer is removed, the strain at measuring position z_m must be measured.

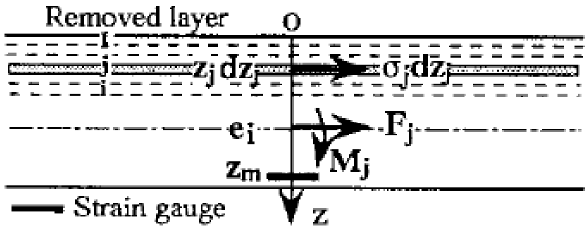

Fig. 4 Schematic showing of layer removal method

(3) Measuring equations

When i layers are removed, the stresses $\sigma_1^L, \sigma_2^L, ..., \sigma_i^L$ of these i layers will be released. If the size of j-th layer $(1 \le j \le i)$ is dz_j and the specimen thickness is unit, the released force on the j-th layer should be $\sigma_j^L dz_j$. This force at the j-th layer can be expressed by the force F_j and the moment M_j acting on a neutral axis.

$$\begin{aligned} F_j &= \sigma_j^L dz_j, \\ M_j &= F_j(e_i - z_j) = \sigma_j^L dz_j(e_i - z_j), \qquad (j = 1 \sim i) \end{aligned} \tag{2}$$

Where, e_i and z_i are the coordinate of the neutral axis after i layers are removed and coordinate of the j-th layer, respectively.

After i layers are all removed, the axial force F and moment M acting on the neutral axis can be calculated by **Eq. (3)**.

$$\begin{aligned} F &= \sum_{j=1}^{i} F_j = \sum_{j=1}^{i} \sigma_j^L dz_j \\ M &= \sum_{j=1}^{i} F_j(e_i - z_j) = \sum_{i=1}^{i} \sigma_j^L dz_j(e_i - z_j) \end{aligned} \tag{3}$$

If the measured strain at position z_m is ε_i^m after i layers are removed, the relation between measured strain ε_i^m and released stresses σ_j^L (j=1～i) can be derived by elastic beam theory.

$$\begin{aligned} \varepsilon_i^m &= \frac{F}{(h - z_i - dz_i/2)E_m} - \frac{M(z_m - e_i)}{(EI)_i} \\ &= \frac{\sum_{j=1}^{i} \sigma_j^L dz_j}{(h - z_i - dz_i/2)E_m} - \frac{(z_m - e_i)\sum_{j=1}^{i} \sigma_j^L dz_j(e_i - z_j)}{(EI)_i} \end{aligned} \tag{4}$$

where, h, z_m, E_m are the thickness of the clad plate, the coordinate and Young's modulus of the material at the strain gauge position, respectively. $(EI)_i$ is bending stiffness of the beam after i layers are removed.

If **Eq. (4)** is written in vector form, the following equations can be created.

$$\varepsilon_i^m = \{c_{i1}, c_{i2}, ..., c_{ii}\}\{\sigma_1^L, \sigma_2^L, ..., \sigma_i^L\}^T \tag{5}$$

$$c_{ij} = \frac{\sigma_j^L dz_j}{(h - z_i - dz_i/2)E_m} - \frac{\sigma_j^L dz_j (z_m - e_i)(e_i - z_j)}{(EI)_i}, \quad (1 \le j \le i) \tag{6}$$

If, totally, q layers are removed in the experiment and the strain is measured after each layer is removed, the following equations can be obtained.

$$\begin{aligned} &i = 1, \quad \varepsilon_1^m = \{c_{11},\ 0, ..., 0\}\{\sigma_1^L, \sigma_2^L, ..., \sigma_q^L\}^T \\ &i = 2, \quad \varepsilon_1^m = \{c_{21}, c_{22}, ..., 0\}\{\sigma_1^L, \sigma_2^L, ..., \sigma_q^L\}^T \\ &\cdots\cdots\cdots\cdots\cdots \\ &i = q, \quad \varepsilon_1^m = \{c_{q1}, c_{q2}, ..., 0\}\{\sigma_1^L, \sigma_2^L, ..., \sigma_q^L\}^T \end{aligned} \tag{7}$$

If **Eq. (7)** is written in the form of a matrix, the following measuring equation can be obtained.

$$[C]_{q \times q}\{\sigma^L\}_q = \{\varepsilon^m\}_q \tag{8}$$

where, $[C]$ is the elastic response matrix between measured strains and released stresses by the layer removal method.

2.3 Rolling residual stresses in a clad plate (SUS304/MB410)

The measured rolling stresses (σ_x, σ_y) and their distributions through the thickness of the clad plate are shown in **Fig. 5**. The marks (●, ○) are the stresses (σ_x, σ_y) directly measured by strain gauges using conventional stress release methods. The overall distribution of residual stresses measured by the layer removal method agrees well with that by the conventional stress release method. The maximum stress values on the surfaces and the clad interface by the layer removal method are larger than those by the conventional stress release method.

Two stress components (σ_x, σ_y) have a similar distribution shape and are slightly different in their values. The rolling stresses (σ_x, σ_y) are tensile on the SUS304 layer and lower surface of MB410 layer. The local stresses (σ_x, σ_y) at the clad interface are tensile on the side of SUS304 and compressive on the side of MB410.

2.4 Rolling residual stresses in a stainless plate (SUS304)

The rolling residual stresses in a SUS304 plate measured by the conventional stress release method are shown in **Fig. 6**. The rolling residual stresses σ_x and σ_y are compressive on the top surface and bottom surface of the SUS304 plate. They are quite different from the stresses in the SUS304/MB410 clad plate shown in **Fig. 5**.

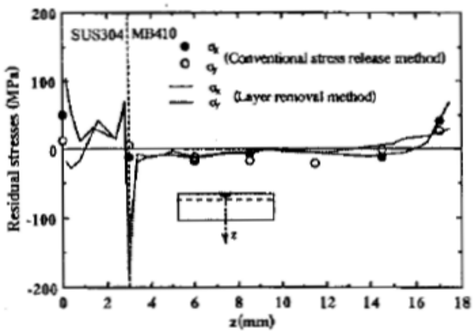

Fig. 5 Rolling stresses in a clad plate

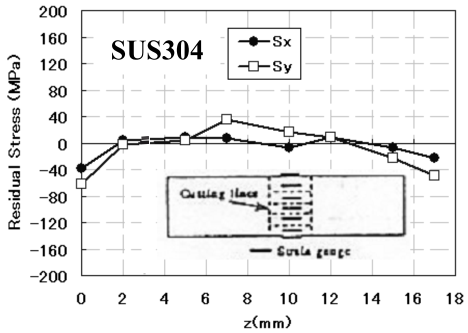

Fig. 6 Rolling stresses in a stainless plate

3. Measurement of welding residual stresses in a bead-on-plate weld

3.1 Inherent strain method for welding residual stress measurement[2-10]

(1) Assumption of inherent strain method

A bead-on-plate weld of 1000mm in length, 500mm in width and 18mm in thickness is shown in **Fig. 7 (a)**. The distribution of welding residual stresses and inherent strains can be assumed to be uniform in the weld line direction except the two ends of weld. In the other words, the stress components and inherent strain components existing in the middle transverse section are only $\sigma_x, \sigma_y, \sigma_z, \tau_{yz}$ and $\varepsilon_x^*, \varepsilon_y^*, \varepsilon_z^*, \gamma_{yz}^*$.

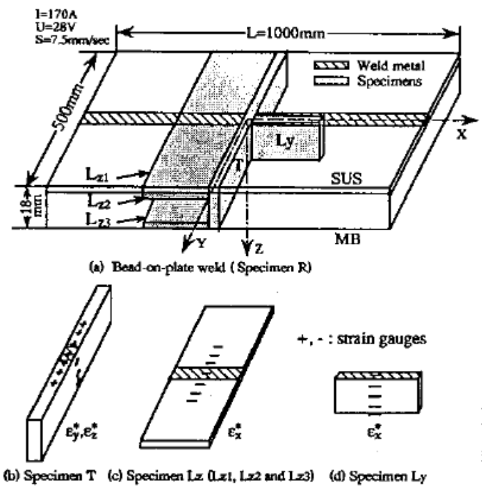

Fig. 7 Bead-on-plate weld and specimens for residual stress measurement

(2) Measuring equations of inherent strain method

The general relationships among inherent strain $\{\varepsilon^*\}$, elastic strain $\{\varepsilon^e\}$ and welding residual stress $\{\sigma\}$ can be expressed by the following equations,

$$[H]\{\varepsilon^*\} = \{\varepsilon^e\} \tag{9}$$

$$\{\sigma\} = [D]\{\varepsilon^e\} \tag{10}$$

Where, $[H]$ is the elastic response matrix between inherent strain and elastic strain and $[D]$ is elastic stress-strain matrix of material defined by Young's modulus and Poisson's ratio.

Equations (9-10) for all specimens shown in **Fig. 7** have the same form. The value of elastic strains $\{\varepsilon^e\}$ and the components H_{ij} of matrix $[H]$ will be different between the specimens. The elastic strain $\{\varepsilon^e\}$ in each specimen can be measured. The matrix $[H]$ for each specimen can be created by elastic FEM computation. The component H_{ij} is equal to the elastic strain at the measuring element when unit inherent strain is applied to the FEM model as an initial strain.

(3) Separation of inherent strain components

To measure welding stresses in the transverse section using the inherent strain method, one piece of T-specimen (transverse section specimen), three pieces specimens Lz (L_{z1}, L_{z2}, L_{z3}) and one piece specimen Ly as shown in **Figs. 7 (a)**, **(b)** and **(c)** are cut off from the original bead-on-plate weld. The specimens Lz1, Lz2 and Lz3 are used for the stress measurements on SUS304 layer, MB410 layer and bottom layer of the clad plate, respectively. The strain gauges attached on each specimen are schematically represented in the figures. The inherent strain components existing in specimen T and in specimens Lz, Ly are, $\{\varepsilon_y^*, \varepsilon_z^*, \gamma_{yz}^*\}$ and ε_x^*, respectively, which are the same as those in the original bead-on-plate weld. The welding residual stresses $\{\sigma\}$ can be divided into two parts $\{\sigma^A\}$ and $\{\sigma^B\}$ as shown in **Eq. (11)**, which are produced by the transverse inherent strain components ($\varepsilon_y^*, \varepsilon_z^*, \gamma_{yz}^*$) and the longitudinal component ε_x^* in the welding direction (x), respectively.

$$\begin{aligned}\{\sigma\} &= \{\sigma(\varepsilon_y^*, \varepsilon_z^*, \gamma_{yz}^*)\} + \{\sigma(\varepsilon_x^*)\} \\ &= \{\sigma^A\} + \{\sigma^B\}\end{aligned} \tag{11}$$

3.2 Welding residual stresses $\{\sigma^A\}$ due to inherent strains ($\varepsilon_y^*, \varepsilon_z^*, \gamma_{yz}^*$)

If the overall distribution inherent strains ($\varepsilon_y^*, \varepsilon_z^*, \gamma_{yz}^*$) are measured in the specimen T, the overall distribution of residual stresses $\{\sigma^A\}$ can be estimated. If the residual stresses only at the particular positions are necessary, the residual stresses $\{\sigma^A\}$ can be determined by transferring the measured stresses $\{\sigma^T\}$ on specimen T to the original welded joint using following equation.

$$\sigma_x^A = \frac{\upsilon\sigma_y^T + \upsilon\sigma_z^T}{1-\upsilon^2},\ \sigma_y^A = \frac{\sigma_y^T + \upsilon\sigma_z^T}{1-\upsilon^2},$$
$$\sigma_z^A = \frac{\sigma_z^T + \upsilon\sigma_y^T}{1-\upsilon^2},\ \tau_{yz}^A = \frac{\tau_{yz}^T}{1-\upsilon^2} \tag{12}$$

where, υ is Poisson's ratio.

The residual stresses $\{\sigma^A\}$ and their distributions on the SUS304 surface (y) and through thickness (z) are shown in **Fig. 8**. The transverse residual stress σ_y^A is tensile on both the top surface and the bottom surface of the weld zone. The value of transverse residual stress σ_y^A is larger than the values of longitudinal residual stress σ_x^A and residual stress σ_z^A in thickness direction.

3.3 Welding residual stresses $\{\sigma^B\}$ due to inherent strain ε_x^*

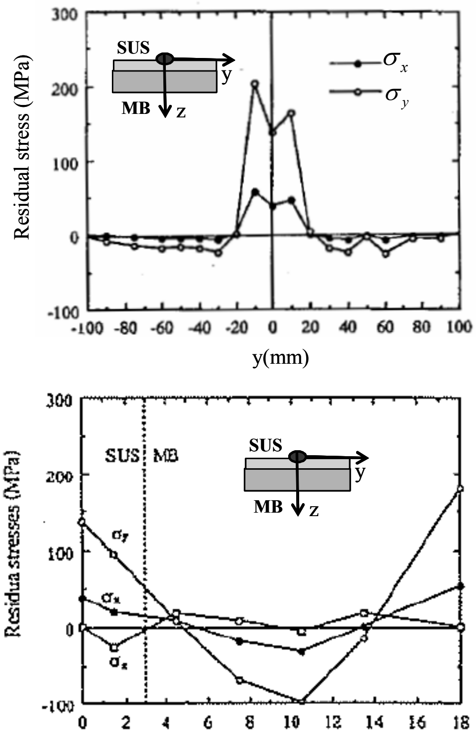

Fig. 8 Welding residual stresses $\{\sigma^A\}$ due to inherent strains $\varepsilon_y^*, \varepsilon_z^*, \gamma_{yz}^*$

To estimate the distribution of residual stresses $\{\sigma^B\}$ by the inherent strain method, the distribution of inherent strain ε_x^* has to be determined. The inherent strain distribution in the transverse direction (y) and in the thickness direction (z) can be estimated by **Eq. (9)** using the measured elastic strain ε_x^e in Ly and Lz specimens.

The measured residual stress $\sigma_x^{Lz}(=E\times\varepsilon_x^e)$ in specimens Lz (L_{z1},L_{z2},L_{z3}) and its distribution in the y-direction are shown in **Fig. 9** by marks ●, ○, □. The parameters a_1,a_2,a_3 shown in **Fig. 9** are the half width of inherent strain zone in the y-direction, which are corresponding to the positions of the peak compressive residual stresses in the y-direction of the specimens L_{z1},L_{z2},L_{z3}, respectively. The width of inherent strain zone can be expressed by $a(z)$, where z is the z-coordinate. The distributions of inherent strain ε_x^* in the y-direction of specimens (L_{z1},L_{z2},L_{z3}) estimated by **Eq. (9)** are shown in **Fig. 10**, which has a simple distribution shape compared with the residual stress σ_x. The reproduced residual stresses in specimens L_{z1},L_{z2},L_{z3} by inherent strain ε_x^* are also plotted in **Fig. 9**. The residual stresses are accurately reproduced by the inherent strain method.

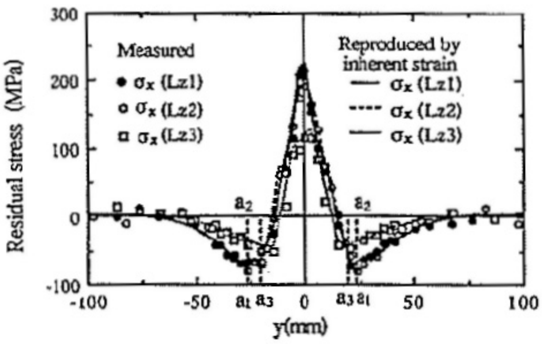

Fig. 9 Residual stresses in L_{z1},L_{z2},L_{z3}

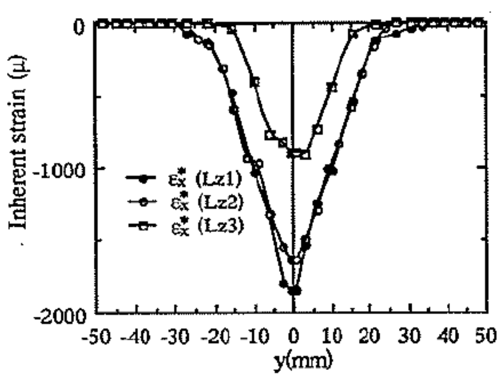

Fig. 10 Inherent strain in y-direction

The distribution of inherent strain ε_x^* in the z-direction of specimen Ly consists of a linear part $\varepsilon_{xL}^*(z)$ and a non-linear part $\varepsilon_{xN}^*(z)$ described as below,

$$\begin{aligned}\varepsilon_x^*(z) &= \varepsilon_{xL}^*(z)+\varepsilon_{xN}^*(z)\\ &= c_1+c_2z+\varepsilon_{xN}^*(z)\equiv\varepsilon_x^*(0,z)\end{aligned} \quad (13)$$

where, c_1 and c_2 are the coefficients of linear inherent strain $\varepsilon_{xL}^*(z)$.

The linear inherent strain $\varepsilon_{xL}^*(z)$ is equal to the released strain when specimen Ly is cut off. It can be measured by attaching the two strain gauges respectively on the top surface and the bottom surface of specimen Ly before cutting off from the original bead-on-plate weld.

The non-linear part $\varepsilon_{xN}^*(z)$ is equal to the released strain, which can be measured by attaching new strain gauges on the specimen Ly. The measured inherent strains $\varepsilon_{xL}^*(z)$, $\varepsilon_{xN}^*(z)$ and their distributions in the thickness direction (z) are shown in **Fig. 11**.

To determine the distribution of welding residual stresses $\{\sigma^B\}$, the distribution of inherent strain ε_x^* has to be known. Here, a function defined by **Eq. (14)** is adapted to describe the inherent strain distribution on the transverse section,

$$\begin{aligned}\varepsilon_x^*(y,z) &= \varepsilon_x^*(0,z)[1-\frac{y}{a(z)}][1+A_1(\frac{y}{a(z)})+A_2(\frac{y}{a(z)})^2]\\ &= [c_1+c_2z+\varepsilon_{xN}^*(z)][1-\frac{y}{a(z)}][1+A_1(\frac{y}{a(z)})+A_2(\frac{y}{a(z)})^2]\end{aligned} \quad (14)$$

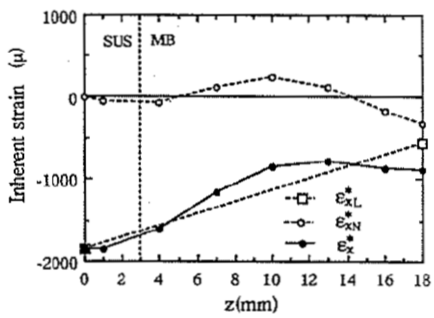

Fig. 11 ε_x^* distribution in z-direction

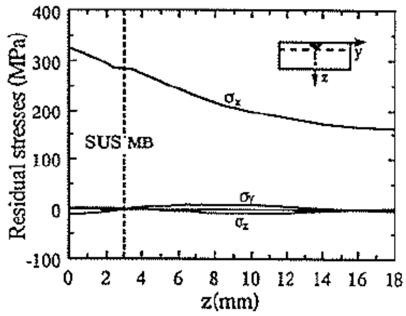

Fig. 12 Welding residual stresses $\{\sigma^B\}$ due to ε_x^*

where, $a(z)$ is the half width of the inherent strain zone and varies slightly in the z-direction. Coefficients A_1 and A_2 can be determined by function fitting using inherent strains already measured in specimens L_{z1}, L_{z2}, L_{z3} as shown in **Fig. 10** and **Fig. 11**. **Figure 12** shows the residual stresses $\{\sigma^B\}$ and their distributions through thickness estimated by applying inherent strain ε_x^* expressed by **Eq. (4)** to the original bead-on-plate weld. As shown in **Fig. 12**, the residual stress σ_x is dominantly larger compared with the residual stress components σ_y and σ_z.

3.4 Welding residual stresses in original bead-on-plate weld

The residual stresses, sum of $\{\sigma^A\}$ and $\{\sigma^B\}$, and their distributions along the SUS304 surface (y) and through thickness (z) are shown in **Fig. 13**. $\sigma_x(weld), \sigma_y(weld), \sigma_y(weld)$ in **Fig. 13** are the welding residual stresses only. The marks ●, ○, □ are the total residual stresses, the sum of welding residual stresses and rolling residual stresses. The welding residual stress $\sigma_x(weld)$ is tensile overall the thickness. The welding residual stress $\sigma_y(weld)$ is tensile on the top surface and bottom surface of the welded zone. The welding residual stress $\sigma_z(weld)$ is very small. The residual stress state is two directional tensile on the surfaces of the weld zone.

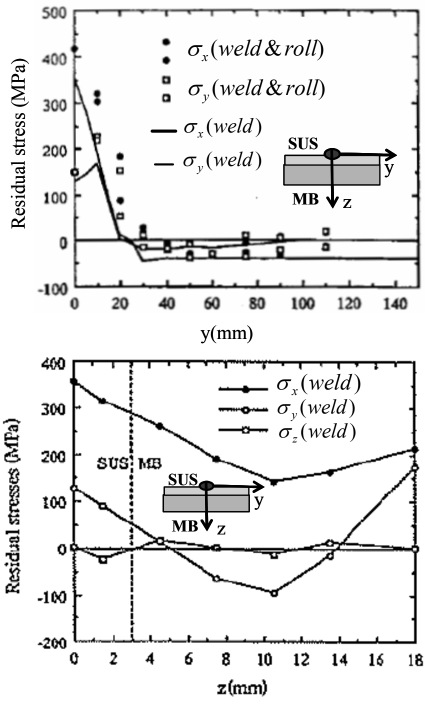

Fig. 13 welding residual stress distributions through thickness direction (z)

The total tensile residual stresses (●, ○, □) on the SUS304 surface shown **Fig. 13** have larger tensile values than those of welding stresses because the in-rolling residual stresses are tensile on the surface of the clad plate.

4. Measurement of residual stresses in fillet welds with clad plates

4.1 Fillet welded joint

Figure 14 (a) shows a fillet welded joint with a clad plate (SUS304/MB410) and a stainless plate (SUS304). To measure the welding residual stress, specimen T and specimens Lz (Lz1, Lz2, Lz3), Ly shown in **Fig. 14 (b)** and **Fig. 14(c)**, respectively, are prepared[8-10].

4.2 Separation of inherent strain components and residual stresses

By cutting off the specimen T and the specimens L_{z1}, L_{z2}, L_{z3}, L_y, the inherent strain components $\varepsilon_x^*, \varepsilon_y^*, \varepsilon_z^*, \gamma_{yz}^*$ in the original fillet welded joint can be separated into two parts, which are transverse components $(\varepsilon_y^*, \varepsilon_z^*, \gamma_{yz}^*)$ in specimen-T and longitudinal component ε_x^* in specimens L_{z1}, L_{z2}, L_{z3}, Ly, respectively. Therefore, the residual stresses can be divided into two parts $\{\sigma^A\}$ and $\{\sigma^B\}$, which are produced by the transverse inherent strain components ($\varepsilon_y^*, \varepsilon_z^*, \gamma_{yz}^*$) and the component ε_x^* in welding direction (x), respectively.

4.3 Measurement of residual stresses $\{\sigma^A\}$ by inherent strains $(\varepsilon_y^*, \varepsilon_z^*, \gamma_{yz}^*)$

The welding residual stresses $\{\sigma^A\}$ measured in specimen-T and transferred by **Eq. (12)** are shown in **Fig. 15**. A large tensile stress σ_y near the fillet weld zone on the surface of SUS304 layer of clad flange can be observed in **Fig. 15 (a)**. A large tensile stress σ_z occurs at the SUS304 side of the SUS304/MB410 interface.

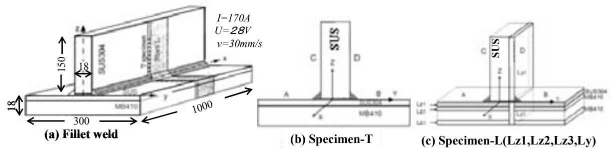

Fig. 14 A fillet weld and specimens for measurement of welding residual stresses

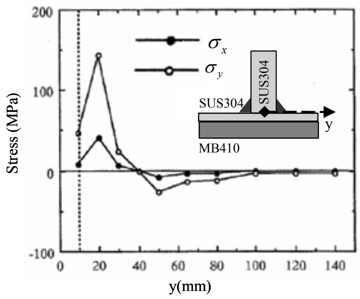

(a) Stress distribution in y-direction.

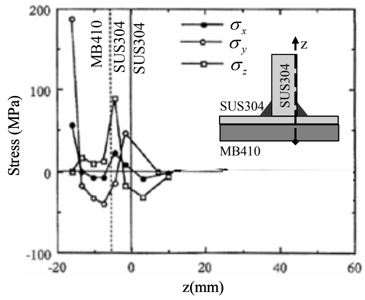

(b) Stress distribution in z-direction

Fig. 15 Welding residual stresses $\{\sigma^A\}$ due to inherent strain $\varepsilon_y^*, \varepsilon_z^*, \gamma_{yz}^*$

4.4 Measurement of residual stresses $\{\sigma^B\}$ by inherent strain ε_x^*

Inherent strain ε_x^* and its distribution in specimens $L_{z1}, L_{z2}, L_{z3}, Ly$ can be estimated by **Eq. (9)** using measured elastic strain in these specimens. The inherent strain ε_x^* distributing in flange and web of the middle transverse section can be separately expressed by the functions defined as below,

In flange $$\varepsilon_x^*(y,z) = \sum_{i=1}^{M}\sum_{j=1}^{N} A_{ij}^*(1-\frac{y}{a})^i(1-\frac{z}{b})^j \quad (15)$$

In web $$\varepsilon_x^*(y,z) = \sum_{j=1}^{N} A_j^*(1-\frac{z}{b})^j \quad (16)$$

Where, a (=35mm) is the half width of the inherent strain zone in the flange and b (=30mm) is the width of the inherent strain zone in the web. Coefficient A_{ij}^*, A_j^* can be predicted by function fitting using inherent strains already measured in specimens L_{z1}, L_{z2}, L_{z3} and Ly.

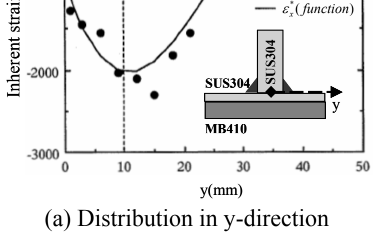

(a) Distribution in y-direction

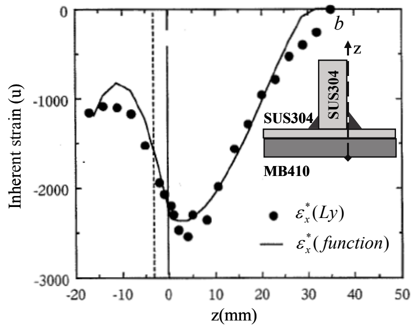

(b) Distribution in z-direction

Fig. 16 Inherent strain distribution expressed by function and measured in Lz1 and Ly

The distribution of inherent strain ε_x^* expressed by **Eq. (15)** and **Eq. (16)** with M=N=3 are shown in **Figs. 16(a)** and **(b)**, respectively. The marks ● show the values of inherent strain directly measured in specimens Lz1 and Ly.

Figure 17 shows the welding residual stresses $\{\sigma^B\}$ due to inherent strain ε_x^* expressed by **Eq. (15)** and **Eq. (16)**.

4.5 Residual stresses in fillet welded joint

The welding residual stress distributions $\sigma(weld)$ in y-direction and z-direction measured in a fillet welded joint by the inherent strain method are shown in **Figs. 18 (a)** and **(b)**, respectively. The marks ●,○,■,□ and $\sigma(weld\,\&\,roll)$ in **Fig. 18** are the total residual stresses, sum of rolling residual stresses and welding residual stresses on the surfaces of flange and web measured by strain gauges directly[11]. The welding

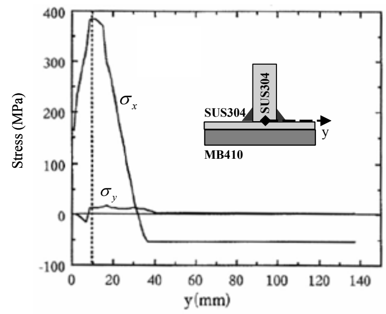

(a) Distribution in y-direction

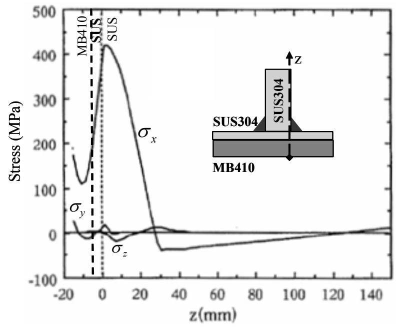

(b) Distribution in z-direction

Fig. 17 Welding residual stresses $\{\sigma^B\}$ due to inherent strain ε_x^*

residual stresses (σ_x, σ_y) are tensile in the fillet weld zone and compressive away from the weld zone.

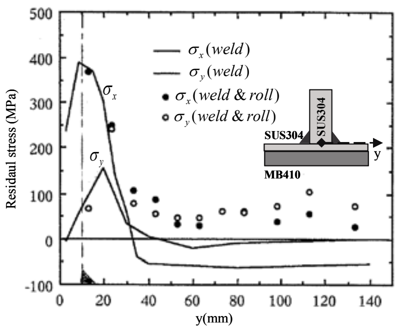

(a) Distribution in y-direction

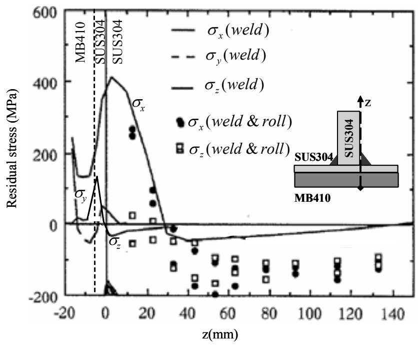

(b) Distribution in z-direction

Fig. 18 Welding Residual stresses and rolling residual stresses in fillet weld with clad plate

However, the total residual stresses $\sigma_x(weld \& roll)$ and $\sigma_y(weld \& roll)$ away from the weld zone on the SUS304 surface of SUS304/MB410 clad flange are tensile. This is because the rolling residual stresses on SUS304 layer are tensile. The total residual stresses $\sigma_x(weld \& roll)$ and $\sigma_z(weld \& roll)$ away from the weld zone on SUS304 web are compressive. This is because the rolling residual stresses on the surface of SUS304 web are compressive. Therefore, the fillet weld zone and SUS304 surface of the clad plate may be weaker in resisting stress corrosion. To improve the corrosion resistance of SUS/MB clad steel, a higher grade of stainless steel is recommended.

5 Conclusions

(1) Layer removal method is proposed and adapted for the measurement of rolling residual stresses in the SUS304/MB410 clad plate.
(2) Rolling residual stresses are tensile on the SUS304 layer of the SUS304/MB410 clad plate,
(3) Rolling residual stresses are compressive on the surface of the SUS304 stainless plate.
(4) Welding residual stresses are tensile in the weld zone of bead-on-plate weld and fillet weld.
(5) The total residual stresses, sum of rolling residual stresses and welding residual stresses, are tensile on the SUS304 layer of the SUS304/MB410 clad plate after bead–on-plate welding and fillet welding.

References

1) Y.Ueda H. Murakawa, N.X.MA : Measuring Method for Residual Stresses in Explosively Clad Plates and a Method of Residual Stress Reduction, Trans. ASME, J. Engineering Materials and Technology, Vol.118(1996), p567-582.
2) YukioUeda, Hidekazu Murakawa and Ninshu Ma : Computational Approach to Welding Deformation and Residual Stress (in Japanese), Sanpo-pub, Oct.,2007, ISBN978-4-88318-033-2
3) Y.Ueda, K.Fukuda : New Measuring Method of Three Dimensional Residual Stresses in Long Welded Joints Using Inherent Strains as Parameters – Lz Method--, Trans. ASME, J. Engineering Materials and Technology, Vol.111(1989),p1-8.
4) Yukio UEDA and Ning Xu MA: A Function Method for Estimating Inherent Strain Distributions, Trans. JWRI, Vol.23, No.1, 1994, p.71-78
5) Yukio Ueda and Ning Xu Ma: Expression of Inherent Strain in Form of Function and its Estimation, Quarterly Journal of the Japan Welding Society, Vol.11, No.1, 1993, p189-195 (In Japanese)
6) Ning Xu MA and Yukio UEDA : TLyLz-Method and T-Method for Measuring 3-Dimensional Residual Stresses in Bead-on-Plate Welds, Trans. JWRI, Vol.23, No.2, 1994, p.239-247
7) Yukio Ueda, Ning Xu Ma and Ryoichi Koki: TLyLz-Method and T-Method for Measuring 3-Dimensional Residual Stresses in Bead-on-Plate Welds, Quarterly Journal of the Japan Welding Society, Vol.11, No.4, 1993, p555-562 (In Japanese)
8) Yukio UEDA and Ning Xu MA: Distributions of Residual Stresses and Inherent Strains in Fillet Welds, Trans. JWRI, Vol.24, No.2, 1995, p.123-130
9) Yukio Ueda and Ning Xu Ma: Function Expression for Inherent Strains in Fillet Welds and Its Accuracy, Quarterly Journal of the Japan Welding Society, Vol.12, No.4, 1994, p554-560 (In Japanese)
10) Yukio Ueda, Ning Xu Ma, Ya Sheng Wang and Ryoichi Koki: Measurement of Residual Stresses in Single-pass and Multipass Fillet Welds Using Inherent Strains, Quarterly Journal of the Japan Welding Society, Vol.13, No.3, 1995, p470-478 (In Japanese)
11) N. X. Ma, H. Murakawa and Y. Ueda : Effects of Initial Stresses on Welding Deformation and Residual Stresses, Proceedings of 6th International Welding Symposium and Japan Welding Society, The Roles of Welding Science and Technology in the 21 Century, 19-21, Nov., 1996, Nagoya, Japan, Vol.2, pp.557-562